Clinical and Translational Radiation Oncology 9 (2018) 23–29

Contents lists available at ScienceDirect

Clinical and Translational Radiation Oncology

journal homepage: www.elsevier.com/locate/ctro

Original Research Article

Do protons and X-rays induce cell-killing in human peripheral blood lymphocytes by different mechanisms?

J. Miszczyk [a,*], K. Rawojć [b], A. Panek [a], A. Borkowska [a], P.G.S. Prasanna [c], M.M. Ahmed [c], J. Swakoń [a], A. Gałaś [d]

[a] Institute of Nuclear Physics Polish Academy of Sciences, PL-31342, Poland
[b] Department of Endocrinology, Nuclear Medicine Unit, The University Hospital, Kraków, Poland
[c] Radiation Research Program, National Cancer Institute, National Institutes of Health, Bethesda, MD, USA
[d] Department of Epidemiology, Chair of Epidemiology and Preventive Medicine, Jagiellonian University Medical College, Kraków, Poland

ARTICLE INFO

Article history:
Received 25 July 2017
Revised 31 December 2017
Accepted 15 January 2018
Available online 31 January 2018

Keywords:
Proton biology
Human peripheral blood lymphocytes
Cell-killing modes
Apoptosis
Necrosis
Proton therapy
Photon therapy
Radiotherapy

ABSTRACT

Purpose: Significant progress has been made in the technological and physical aspects of dose delivery and distribution in proton therapy. However, mode of cell killing induced by protons is less understood in comparison with X-rays. The purpose of this study is to see if there is any difference in the mode of cell-killing, induced by protons and X-rays in an *ex vivo* human peripheral blood lymphocyte (HPBL) model.

Materials and methods: HPBL were irradiated with 60 MeV proton beam or 250-kVp X-rays in the dose range of 0.3–4.0 Gy. Frequency of apoptotic and necrotic cells was determined by the Fluorescein (FITC)-Annexin V labelling procedure, 1 and 4 h after irradiation. Chip-based DNA Ladder Assay was used to confirm radiation-induced apoptosis and necrosis. Chip-based DNA Ladder Assay was used to confirm radiation-induced apoptosis.

Results: *Ex vivo* irradiation of HPBL with proton beams of 60 MeV or 250 kVp X-rays resulted in apoptotic as well as necrotic modes of cell-killing, which were evident at both 1 and 4 h after irradiation in the whole dose and time range. Generally, our results indicated that protons cause relatively higher yields of cell death that appears to be necrosis compared to X-rays. The analysis also demonstrates that radiation type and dose play a critical role in mode of cell-killing.

Conclusion: Obtained results suggest that X-rays and protons induce cell-killing by different modes. Such differences in cell-killing modes may have implications on the potential of a given therapeutic modality to cause immune modulation *via* programmed cell death (X-rays) or necrotic cell death (proton therapy). These studies point towards exploring for gene expression biomarkers related necrosis or apoptosis to predict immune response after proton therapy.

Introduction

Protons with energies from 60 to 250 MeV are being used in the treatment of certain types of cancer (e.g., paediatric, head and neck, brain, gastrointestinal, lung, genitourinary, eye tumours) [1]. Compared to conventional radiotherapy, they offer better dose delivery and distribution, and thus lower probability of collateral normal tissue damage and lower risk of post-treatment complications [1,2]. Several phase I and II clinical trials are ongoing to explore the advantages of proton therapy over X-rays [2]. The physical properties of proton beams used in therapy have been widely characterized [3]. Despite of the well understood physical aspects of proton therapy, proton biology and its clinical relevance are still less understood [4]. The results of ongoing studies suggest that the biological response following proton irradiation is modulated differently than after X-ray exposure [5]. A deeper understanding of dissimilarity in cell killing induced by proton beams in comparison to photons is necessary. Previously, we characterized the response of Human Peripheral Blood Lymphocytes (HPBL) to therapeutic proton radiation of 60 MeV, by studying the nuclear division index and DNA damage and compared the results with X-rays [6]. A spatial difference in the energy deposition with proton irradiation in comparison to X-rays resulted in a localized manifestation of cytogenetic damage at cellular level [6]. These studies led us to believe that there might be differences in

* Corresponding author at: Department of Experimental Physics of Complex Systems, Institute of Nuclear Physics Polish Academy of Sciences, Radzikowskiego 152 Street, Kraków, PL-31342 Poland.
E-mail address: justyna.miszczyk@ifj.edu.pl (J. Miszczyk).

https://doi.org/10.1016/j.ctro.2018.01.004
2405-6308/

cell-killing modes between protons and photons, due to a difference in the spatial distribution of energy, which might be clinically relevant in evoking or suppressing immune response.

Radiation induces cell-killing through different modes: apoptosis, necrosis, necroptosis, autophagy, senescence, and mitotic catastrophe [7]. Apoptosis and necrosis are two major cell death modes, controlled by different physiological processes and molecular pathways [8]. Generally, irradiation induces apoptosis in most normal cells, but it also occurs in some tumour types [9], and peaks at 3–5 h after irradiation depending on cell type and radiaton dose. Susceptibility to apoptosis is a major determininant of radiosensitivity for most cells [9,10]; higher radiosensitivity of lymphocytes is due to their propensity to apoptosis [11].HPBL are predominantly in a resting phase (G0) of the cell cycle, they are a synchronous and homogeneous cell population, which is in continuous trafficking throughout the body and represent normal tissue. Lymphocytes are involved in many key mechanistic roles following exposure to radiation therapy of tumours, which include, systemic responses at distant sites, enhancement of anti-tumour innate and adaptive immune response, enhanced tumour recognition and killing *via* up-regulation of antigen presenting machinery and induction of positive immunomodulatory pathways due to trafficking of lymphocytes into the tumour microenvironment [12]. It has recently become apparent that particle therapy may distinctly affect cell death pathways, leading to an increased immunogencity [13]. Since proton treatment will minimize exposure of normal tissue [1], thereby exposure of normal lymphocytes in relation to photon irradiation, immunogenecity is likely to be less compared to photons in circulating lymphocytes [13]. Among patients treated with C-ions for esophageal, uterine and cervical cancers in peripheral blood lymphocytes level of cytogenetic damage was lower compared to X-rays [14].

Since HPBL traffic throughout the body, which include irradiation field, could potentially be used to interrogate radiation injury to normal tissue during irradiation of tumours. There is a need to understand the differences in cell-killing mechanisms induced by currently used radiation therapies; not only cell-killing in the tumour tissue but also in normal tissue, since total sparing of normal tissue within the treatment volume is not feasible. In this article, we present the results of our studies that looked at the differences in modes of cell-killing in an HPBL model, which represents the normal tissue, after *ex vivo* irradiation with photons and protons. Also, we discuss the possible mechanistic reasons for these differences, limitations, and potential implications for radiation therapy in light of emerging literature in this rapidly evolving field.

Materials and methods

Blood collection

Whole peripheral blood was collected after obtaining informed consent from healthy, non-smoking donors (3 male and 2 female), aged between 36 and 56 years, in the same conditions as described earlier [6]. Lymphocytes were isolated by density gradient separation using Histopaque®-1077 (Sigma–Aldrich, St. Louis, United States). Cell viability was tested by the trypan blue exclusion test. The number of dye-excluding cells was 100% for all donors. The human bioethical committee of the Regional Medical Board in Krakow approved the informed consent form used in this study (No. 124/KBL/OIL/2013).

Proton and X-ray irradiations and dosimetry

Proton and X-ray irradiation procedures have been previously described in detail [6]. Briefly, HPBL irradiations with X-rays and protons were performed at the Institute of Nuclear Physics, Polish Academy of Sciences (IFJ PAN), Krakow, Poland. After acceleration, proton beam was delivered to the treatment room by a small field horizontal beam line. The parameters of a fully modulated proton beam with Spread Out Bragg Peak (SOBP) were as follows: 30-mm range, 30-mm modulation (measured in water phantom) and field diameter was collimated to the 40-mm lateral diameter. Parameters of the radiation field ensured homogenous distribution of the dose throughout the irradiated samples placed in eppendorf vials in a cell container. At the center of the cell container position, i.e. at the depths 15-mm of the SOBP, the dose-averaged Linear Energy Transfer (LET) was 2.9 keV/μm. Within the sample position in the SOBP the dose-averaged LET ranged from 2.5 keV/μm to 3.8 keV/μm [15]. The proton beam dosimetry was done as described previously [6], according to the TRS-398 protocol recommended by International Atomic Energy Agency [TRS-398] using a reference dosimeter consisting of a PTW TM31010 semiflex ionization chamber and a PTW UNIDOS Webline Electrometer (PTW, Freiburg, Germany). The dosimeter set was calibrated at the IFJ PAN at Theratron 780 Co-60 treatment unit. Lymphocytes were irradiated in 2 ml eppendorf vials (Eppendorf, Hamburg, Germany) with doses: 0.3, 0.5, 0.75, 1.0, 1.5, 2.0, 2.5, 3.0, and 4.0 Gy for protons and X-rays. The cell number was scored in a Bürker chamber and then resuspended in 1.5 ml RPMI 1640 culture medium (PAA Laboratories GmbH, Pasching, Austria). The final concentration of cell suspension was 5×10^4 cells/ml. A specially designed PMMA-Poly (methyl methacrylate) phantom was placed at the irradiation setup isocentre (in the middle of SOBP) and in the centre of the flat beam. The average dose rate was 0.075 Gy/s. For X-ray irradiation, samples from the same donors were irradiated with the same doses as used for proton irradiation with a dose rate of 0.15 Gy/s by a Philips X-ray machine at the same conditions as described previously [6].

Both proton and X-ray irradiations were carried out at room temperature. Post-irradiation incubation of lymphocytes was done at 37 °C in RPMI 1640 culture medium supplemented with 10% heat-inactivated foetal bovine serum (Gibco, Carlsbad, United States). A non-irradiated part of the sample served as control (0.0 Gy).

Apoptosis and necrosis quantification

To quantify apoptosis and necrosis in our *ex vivo* HPBL model; Apoptotic, Necrotic and Healthy Cells Quantification Kit (Biotium, Inc., Hayward, USA) was used. The kit allows simultaneous quantification of apoptotic, necrotic and healthy cells. Identification and discrimination of apoptotic and necrotic cells *in vitro* can be challenging, especially late stage apoptosis from necrosis [16]. Biotium kit cannot distinguish late apoptosis from necrosis. We preferred to use fluorescence microscopy with the Biotium kit over flow cytometry for quantitative measurements of apoptosis and necrosis and then used apoptotic ladder kit for confirmation of apoptosis (see descriptions below). In this test, HPBL were washed in PBS and resuspended in 1X binding buffer, then 5 μl of FITC-annexin V, ethidium homodimer III and Hoechst 33,342 solution was added to each tube and incubated for 15 min at 21 °C in dark. HPBL were then washed 2 times with 1X binding buffer, fixed with 2% formamide, placed on a glass slide and covered with a glass coverslip.

Generally, 4–6 representative fields of at least 100 cells per dose, per time point were analyzed separately from 3 independent triplicates (slides), by two independent scorers using fluorescent microscopy coupled to an image analysis system (MetaSystems™, Altlussheim, Germany), according to the criteria described by Zhang et al. [17]. Experiments and irradiations were repeated twice each. All slides were coded, blinded to scorers. Sample decoding

was done after completing the microscopic evaluation of all slides used for the study to maintain scientific rigor and quality. The results were not statistically different between the slides, repetitions nor scorers; therefore, results are presented as mean values.

Confirmation of apoptosis and necrosis

DNA extraction: The DNA from the HPBL was isolated with a commercial DNA isolation kit as a part of Apoptotic DNA Ladder Kit (Roche, Germany) according to the manufacturer's protocol. Lyophilized apoptotic U937 cells included in the Apoptotic DNA Ladder Kit were used as a positive control.

Separation, sizing and quantification of the dsDNA fragments: The Agilent 2100 Bioanalyzer with Agilent DNA 1000 Kit was used to confirm apoptosis of lymphocytes following irradiation using the extracted DNA as above.

DNA chip preparation: Dilution for the chip run was performed using RNase-Free Water (Invitrogen, LifeTech, Carlsbad, USA). The mean concentration of the DNA was 5.75 μl/ml per sample. The concentration was derived by absorbance measurement performed in the wavelength range of 200–1000 nm by TECAN16 Flat Black instrument with NanoQuant Plates (TECAN Group Ltd., Männedorf, Switzerland). For each sample, irradiated or otherwise, absorbance was measured at: 230, 260, 280 and 310-nm wavelenght. Precisely 1-μl of each eluted sample was loaded directly into the DNA chip and run according to the guidelines provided by the TECAN Group Ltd. The test also included a positive control provided by Apoptotic DNA Ladder and Agilent DNA 1000 Ladder Kits. The results were analyzed by the dedicated software in Agilent 2100 Bioanalyzer.

Statistical analysis

Microsoft Office Excel 2013 was used to analyze all data. OriginPro 2017 (OriginLab Co., Northampton, MA, USA) was used for the graphic representation and statistical analysis of the results. The error bars derived for all data points of apoptotic and necrotic cells represent a mean standard error of five donors. To investigate if the results derived by repetitions, slides, and scorers were comparable, Pearson's correlation coefficient was used. To evaluate the statistical significance of compared results three-sigma limit test was used ($p < 0.05$). The ratios of the percentage of apoptotic vs. necrotic cells were normalized and presented as a box chart.

Results and discussion

Apoptosis and necrosis visualisation

Ex vivo irradiation of HPBL with proton beams of 60 MeV or X-rays results in apoptotic as well as necrotic modes of cell-killing. Fig. 1 shows representative images of lymphocytes after *ex vivo* irradiation with 3.0 Gy protons, in both time points: after 1 h or 4 h following staining with Apoptotic, Necrotic and Healthy Cells Quantification Kit (a), compared with representative photos used for HPBL control quantification (0 Gy, (b)), and HPBL after *ex vivo* irradiation with 4.0 Gy X-rays (c), and 4.0 Gy protons (d). Apoptotic cells appear as green, necrotic cells as red and viable cells as blue

The Biotium assay is based on the principle that during apoptosis, phosphatidylserine (PS) is translocated from the inner surface of the cell membrane to the outer surface for phagocytic cell recognition for organized removal of the cellular debri [18]. FITC-labelled Annexin is an Annexin V recombinant conjugated to the fluorescin. FITC-annexin V has a high affinity with PS, thus it binds specifically to the cells with the PS localized on their outer surface membrane. After staining, apoptotic cell population shows green fluorescence. In contrastto apoptosis, loss of plasma-membrane integrity characterises necrosis [8]. Necrotic cells are specifically stained with ethidium homodimer III (red fluorescence), which is a highly positively charged nucleic acid probe and is impermeant to live or apoptotic cells. For visualizing the entire cell population membrane-permeant blue fluorescent DNA dye Hoechst 33,342 is used.

Confirmation of microscopic observation of cell death in HPBL by the DNA fragmentation assay (Agilent DNA 1000 kit)

There is a strong relationship between radiation-induced DNA fragmentation and apoptosis in HPBL. While radiation induces a spectrum of qualitatively different types of DNA lesions (including sizes of 180–200 bp or size multiples of 180–200 bp reflecting apoptosis), apoptotic DNA fragmentation increases in a dose dependent manner [19]. In our studies DNA fragmentation assay was performed to find out whether or not radiation-induced fragmented genomic DNA reflects apoptosis. DNA fragmentation is typically analysed by agarose gel electrophoresis. Agilent DNA 1000 kit is superior to conventional agarose gel electrophoresis as it is more sensitive, has a relatively lower threshold level of detection and allows analysis of sizes of DNA fragments and quantifiable [20,21]. During apoptosis, the activation of specific calcium-dependent endonucleases results in DNA fragmentation of 180–200 bp and with distinct bands of various sizes of multiples of 180–200 bp [22,23]. Representative samples irradiated with protons at doses of: 0.3; 0.5; 1.0; 2.0; 3.0 and 4.0 Gy showing various degrees of DNA fragmentation, are shown in Fig. 2.

Unirradiated sample (D-0) displayed an overall smaller DNA signal and showed no indication of laddering of 180–200 bp or size multiples of apoptotic DNA. Lanes D-0.5 – D-4.0 shows DNA laddering indicative of apoptosis, as well as some smearing indicative of necrosis after different doses of proton irradiation; thus, we speculate the possibility of necrosis by proton irradiation. As known, apoptosis is characterized by a series of dramatic cellular perturbations that not only contribute to cell death but also prepares organized removal of cellular debris by phagocytosis, preventing unwanted immune responses [12]. In contrast, necrosis is characterized by the loss of cell membrane integrity and uncontrolled release of products of cell death into the extracellular space [24].

Quantification studies of apoptosis and necrosis

Percentage of apoptotic and necrotic cells were quantified using the Apoptotic, Necrotic and Healthy Cells Quantification Kit, as described in the Materials and Methods section, and the data are presented in Figs. 3 and 4.

Our results demonstrate that protons are more efficient in cell-killing, which is most likely due to the production of more irreparable lesions compared to X-rays, which agrees with our previous observations [6]. Generally, *ex vivo* exposure to protons in the dose-range 0.3–4.0 Gy resulted in a significantly higher number of necrotic cells compared to X-rays after 1 and 4 h of irradiation ($p < 0.001$; Figs. 3 and 4). However, at lower proton doses of 0.5 and 0.75 Gy, 1 h after irradiation, and at 0.3 Gy after 4 h of irradiation, the observed increases were not significantly higher compared to X-rays. In addition, observed differences in necrotic cells between two radiation types were mostly seen at higher doses (1.5 Gy and above). Necrosis in unirradiated cells was 7.1 ± 1.2%. After 1 h post-irradiation, at a dose of 4.0 Gy, the frequency of necrotic cells increased to 15.2 ± 3.5% with X-rays, and 52.6 ± 12. 9% with protons, an approximate 3-fold increase compared to X-rays. After 4 h of irradiation, the highest number of necrotic cells was observed at doses of 2.5 Gy with protons (48.6 ± 10.4) and at 2.0 Gy for X-rays (21.9 ± 6.4). Above these doses, decline in the fre-

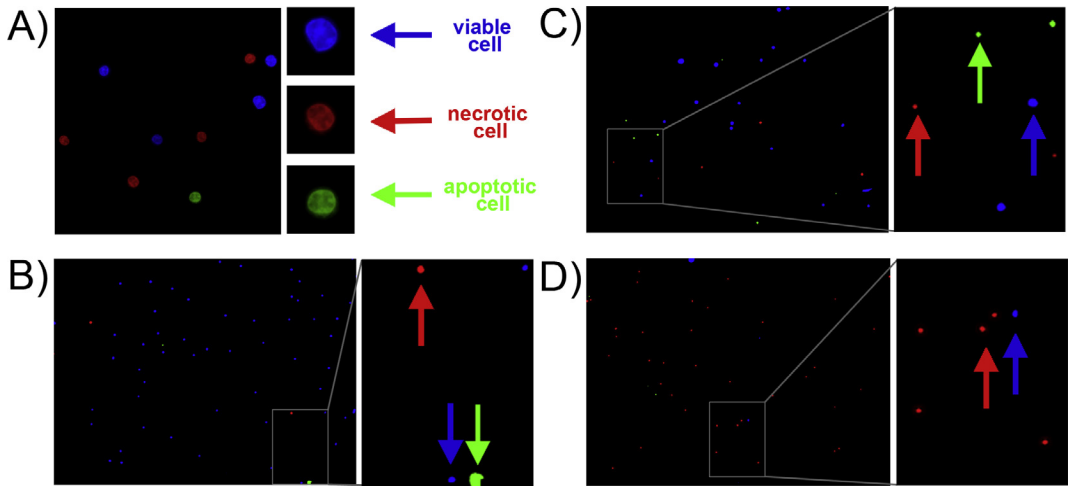

Fig. 1. Representative photomicrographs of HPBL after *ex vivo* irradiation with 3.0 Gy protons following staining with Apoptotic, Necrotic and Healthy Cells Quantification Kit (a, photo: 100× magnification, insert: 250× magnification) compared with representative photos (20× magnification, insert: 60× magnification) used for quantification of control HPBL (0 Gy, b) and HPBL after *ex vivo* irradiation with 4.0 Gy X-rays (c) and 4.0 Gy protons (d). Presented photos were obtained 1 h post irradiation for donor No. 5. Viable (blue, marked by blue arrows), necrotic (red, marked by red arrows) and apoptotic (green, marked by blue arrows) cells were observed under a fluorescent microscope. (For interpretation of the references to colour in this figure caption, the reader is referred to the web version of this article.)

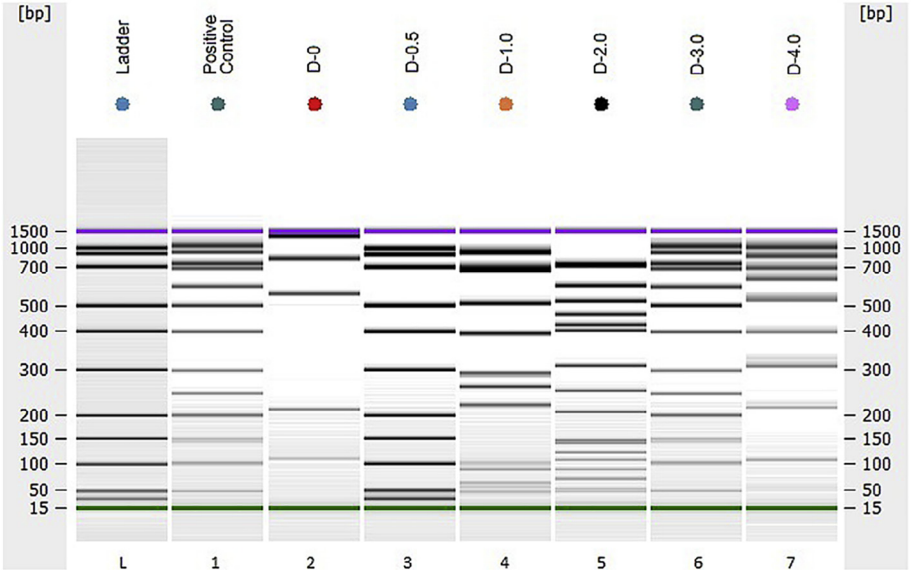

Fig. 2. Confirmation of the microscopic observation of apoptosis by the DNA fragmentation assay. Gel-like image showing positive controls. Ladder, Agilent DNA 1000 Kit; Positive Control, Positive control (U937 cells, Apoptotic DNA Ladder Kit); D-0, control for non-irradiated HPBL; D-0.5 through D-4.0, a display of human DNA from 5 donors irradiated with different doses: 0.5, 1.0, 2.0, 3.0 and 4.0-Gy of protons, respectively (Bioanalyzer 2100 Agilent, USA). With increasing doses of radiation there was a qualitative increase in DNA fragmentation, indicative apoptosis as well necrosis, confirming fluorescence microscopy.

quency of necrotic cells was evident both with protons (30.1 ± 4.1) and X-rays (12.5 ± 1.6), which might be due to dead cells degradation.

Extending these results, we calculated the ratios of apoptotic to necrotic cells after protons and X-ray irradiation at 1 and 4 h post-irradiation timepoints in the studied dose range (Fig. 5).

Median ratios of 14.71 for protons and 24.30 for X-rays were observed for the apoptosis/necrosis ratio after 1 h post-irradiation. Although the difference in the apoptosis/necrosis ratios was relatively small at lower doses of radiation, it was significant at the 4.0 Gy dose ($p < 0.05$). Observed apparent increase in necrotic cells might be due to late occrung apoptosis or more likely necroptosis, since recent studies have shown a co-regulatory interplay between apoptosis and necroptosis [25,26]. The results, although are preliminary, overall confirm the observations that protons induce relatively higher number of necrotic cells compared to apoptosis, especially at higher doses.

These studies on understanding the differences in cell killing mechanisms induced by photons and protons are important because of its potential implications on the possible differences between radiation types to suppress or evoke immune response. Usually tumours that are radiosensitive undergo cell death *via* apoptosis and inactivation of apoptotic machinery is central to the development of cancer [9]. However, induction of mitotic death and cell-killing *via* apoptosis in tumours alone are insufficient to fully explain the therapeutic benefit of radiotherapy [7]. Many other cell types such as cultured fibroblasts (V79, L-929), Chinese hamster ovary (CHO) cells, as well as many human tumour cell lines, do not undergo apoptosis *in vitro* and they generally die *via* necrosis [27]. Immunogenic cell death (ICD) among cancer cells

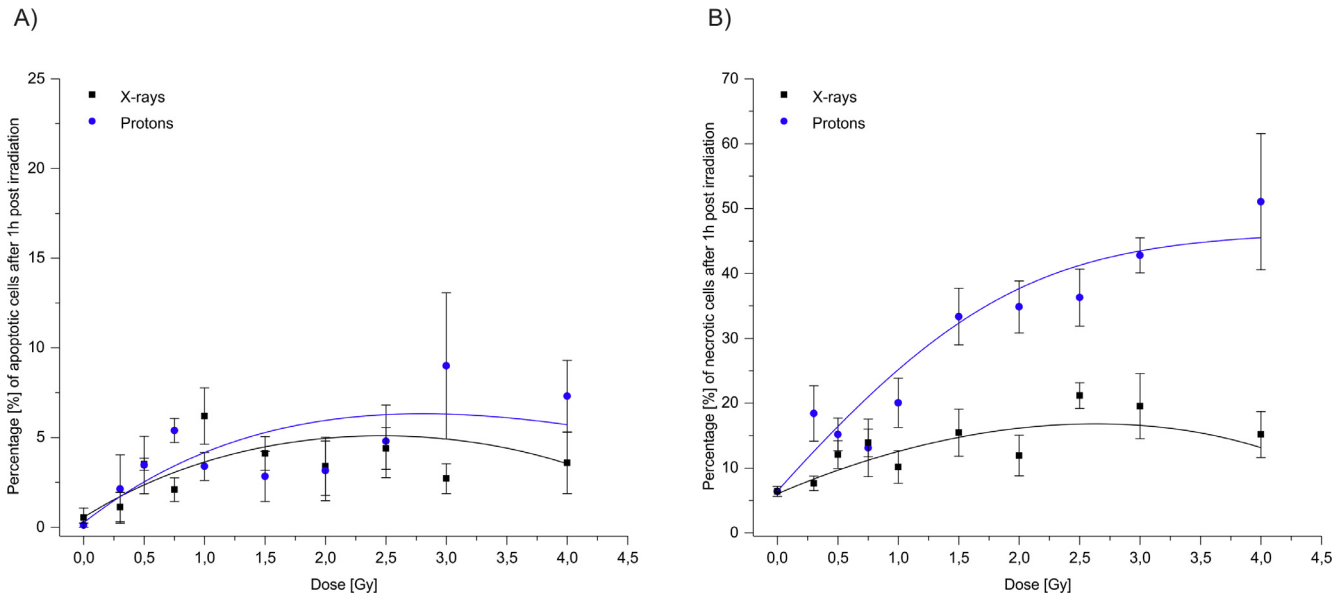

Fig. 3. Percentage of apoptotic (a) and necrotic cells (b) after irradiation with X-rays and protons at 1 h post irradiation at different radiation doses. Cell death was measured using Apoptotic, Necrotic and Healthy Cells Quantification Kit. Error bars represent a standard error of the mean.

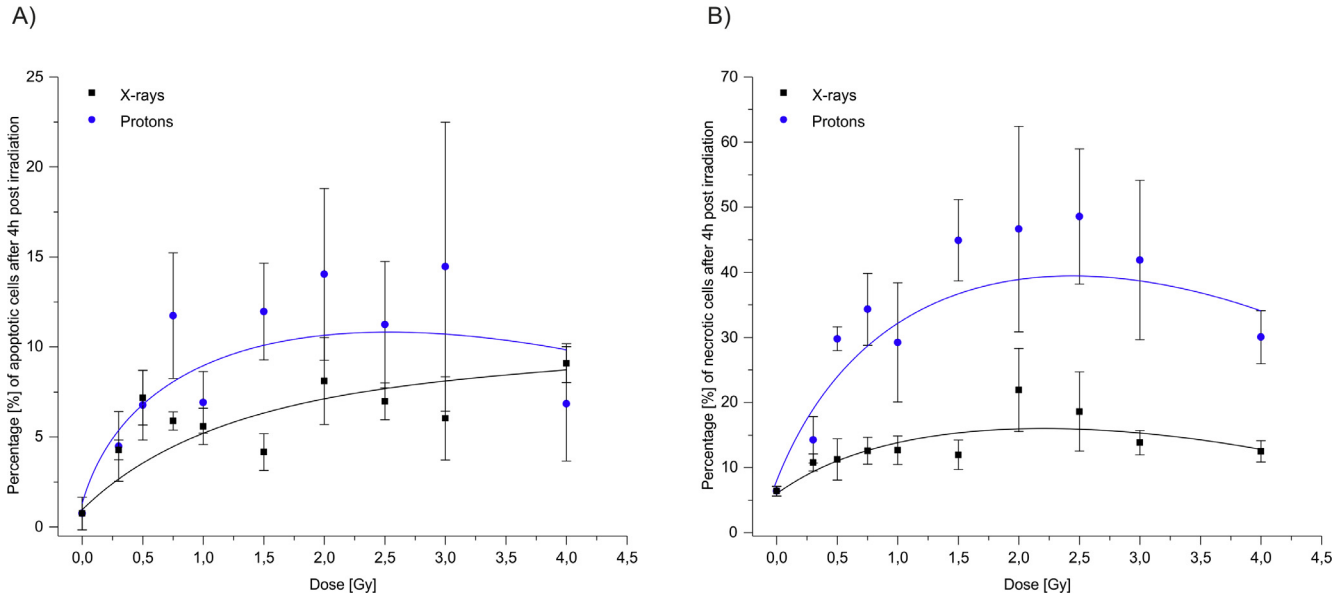

Fig. 4. Percentage of apoptotic (a) and necrotic cells (b) after irradiation with X-rays and protons in lymphocytes 4 h after *ex vivo* irradiation. Cell death was measured using Apoptotic, Necrotic and Healthy Cells Quantification Kit. Error bars represent a standard error of the mean.

constitutes a prominent pathway for the activation of immune system, which involves changes in the composition of cell surface as well as release of soluble mediators, occurring in defined temporal sequence [28]. Inflammatory signalling can occur is *via* necrosis [25] or also *via* secondary necrosis, which occurs when apoptotic cells are not swiftly engulfed by macrophages [29]. The decision between cell survival and death following DNA damage relies on many factors that are involved in DNA damage recognition, DNA repair mechanisms and damage tolerance, as well as on factors involved in the activation of apoptosis, necrosis, necroptosis, autophagy and senescence [30]. At higher doses of therapeutic irradiation, necrosis is also evident [24]. Necrosis of tumor cells will have important bearing in the induction of inflammatory response and potentially local immune activation by spillage of cellular lysate into the circulation [31].

During therapy, protons deposit energy far more selectively to the tumour compared to photons, which is attributed to a higher local tumor control, lower probability of damage of healthy tissue, low risk of complications and the chance for a rapid recovery after therapy [1]. Recent evidences suggest that charged particles may be more immunogenic compared to photons [32]. Recently, it is postulated that charged particles may distinctly affect cell death pathways, leading to increased immunogenicity, and in patients their integral dose likely spare more naive T-cells and memory T-cells, which is essential to direct and sustain a tumor specific immune response [13]. Hence, protons may be more effective in cell-killing due to their potential to cause necrosis in addition to apoptosis. Further, the dose of irradiation also plays a role in modulation of cell death pathways. However, at this time, the published data are fragmentary to conclude whether or not there is a

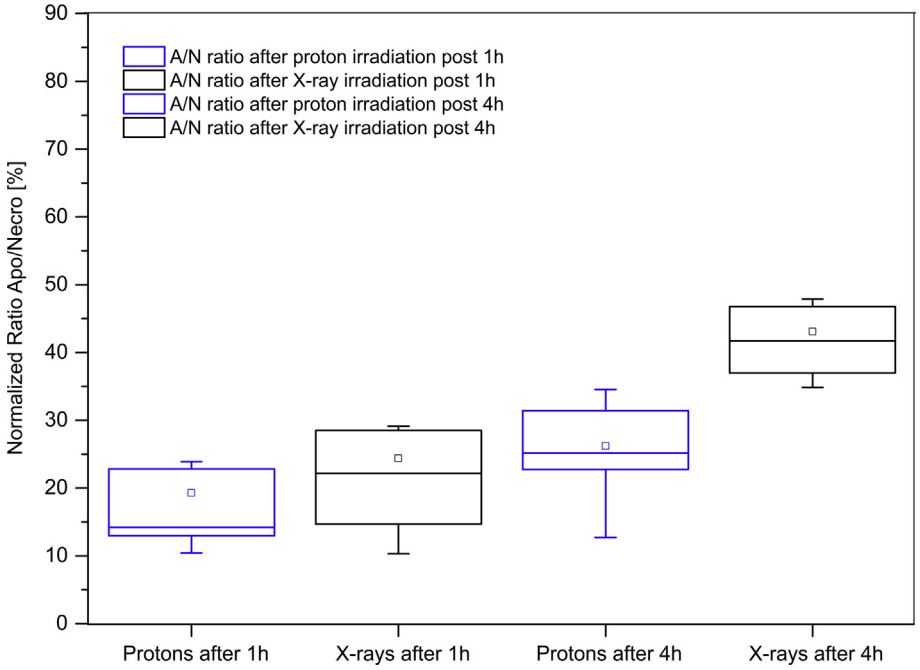

Fig. 5. Normalized ratios of apoptosis/necrosis for protons and X-rays after 1 and 4-h after irradiation in given dose range. Box plot displays variation within the normalized ratios between apoptotic and necrotic cells. The errors taken into consideration are calculated as approximation errors. Spacing between the different parts of the box indicates the degree of spread in the obtained data, showing outliers. The middle horizontal line within the boxes represents median value of each data set.

pivotal dose for determining a specific mode of cell death *vs* the other [10]. Probably in case of the proton beam dose dense energy deposition results in an increase in "*locally multiply damaged sites*" or "*clustered DNA damage*" and consequently, regulated process of apoptosis is inactivated, therefore, cells die mostly by necrosis. This is related to the increased LET with a localized energy deposition resulting in the induction of enhanced, unrepairable biological damage [5].

While our studies on cell killing mode may have important bearing on immune response and possibly treatment [33,34], it is also important to note that our studies are done under *ex vivo* irradiation conditions, where we demonstrate, protons cause relatively more necrosis, which is immunogenic. Further, Apoptotic, Necrotic and Healthy Cells Quantification Kit has its own limitations. Studies have shown that in late apoptotic and necrotic cells, the integrity of the plasma and nuclear membranes decreases, allowing PI to pass through the membranes, intercalate into nucleic acids, leading to problems in distinguishing between these two stages [35,36].

In summary, our studies demonstrate the difference in cell-killing modes induced by X-rays and protons, which may have implications on the potential of a given therapeutic modality to cause robust immune modulation *via* programmed cell death (X-rays) or inflammation (proton therapy). Although our results are preliminary, data from the present studies can guide as a valuable tool in developing appropriate response models to proton therapy. Additionally, HPBL model can serve as a surrogate of normal tissue response to treatment and may allow optimization of treatment planning at an individual patient level. Our studies also point towards exploring gene expression markers related necrosis or apoptosis, which might allow development of biomarkers of immune activation and help improve proton therapy.

Acknowledgments

These investigations were carried out as part of an extended examination of the proton beam at IFJ PAN by cytogenetic and molecular methods and were partially supported by Grant DEC-2013/09/D/NZ7/00324 from the National Science Centre, Poland and under the project co-funded by the Malopolska Regional Operational Program Measure 5.1 Krakow Metropolitan Area as an important hub of the European Research Area for 2007-2013. U.S. National Cancer Institute's (NCI) Radiation Research Program supported Dr. Prasanna's and Dr. Ahmed's assistance. The views expressed are those of the authors; no endorsement by NCI has been given or inferred. Authors gratefully acknowledge the donors for providing blood samples and technical staff for irradiation and dosimetry and "Diagnostics" company in Kraków, Poland for help in blood samples collection. Authors are also grateful for scientific support given by Associate Professor Ewa Stępień from Marian Smoluchowski Institute of Physics, Jagiellonian University in Kraków, Poland and Professor Wojciech M. Kwiatek from Institute of Nuclear Physics Polish Academy of Sciences in Kraków, Poland.

Conflict of interest statement

All authors certify that there is no conflict of interest with any financial organization regarding the material discussed in the manuscript.

References

[1] Loeffler JS, Durante M. Charged particle therapy–optimization, challenges and future directions. Nat Rev Clin Oncol 2013;10:411–24.
[2] Durante M, Orecchia R, Loeffler JS. Charged-particle therapy in cancer: clinical uses and future perspectives. Nat Rev Clin Oncol 2017;14:483–95.
[3] Newhauser WD, Zhang R. The physics of proton therapy. Phys Med Biol 2015;60:155–209.
[4] Girdhani S, Sachs R, Hlatky L. Biological effects of proton radiation: an update. Radiat Prot Dosimetry 2015;166:334–8.
[5] Tommasino F, Durante M. Proton radiobiology. Cancers (Basel) 2015;7:353–81.
[6] Miszczyk J, Rawojc K, Panek A, Swakon J, Prasanna PG, Rydygier M. Response of human lymphocytes to proton radiation of 60 MeV compared to 250 kV X-rays by the cytokinesis-block micronucleus assay. Radiother Oncol 2015;115:128–34.
[7] Eriksson D, Stigbrand T. Radiation-induced cell death mechanisms. Tumour Biol 2010;31:363–72.

[8] Edinger AL, Thompson CB. Death by design: apoptosis, necrosis and autophagy. Curr Opin Cell Biol 2004;16:663–9.
[9] Brown JM, Attardi LD. The role of apoptosis in cancer development and treatment response. Nat Rev Cancer 2005;5:231–7.
[10] Balcer-Kubiczek EK. Apoptosis in radiation therapy: a double-edged sword. Exp Oncol 2012;34:277–85.
[11] Belloni P, Meschini R, Czene S, Harms-Ringdahl M, Palitti F. Studies on radiation-induced apoptosis in G0 human lymphocytes. Int J Radiat Biol 2005;81:587–99.
[12] Park B, Yee C, Lee KM. The effect of radiation on the immune response to cancers. Int J Mol Sci 2014;15:927–43.
[13] Durante M, Brenner DJ, Formenti SC. Does heavy ion therapy work through the immune system? Int J Radiat Oncol Biol Phys 2016;96:934–6.
[14] Durante M, Yamada S, Ando K, Furusawa Y, Kawata T, Majima H, et al. X-rays vs. carbon-ion tumor therapy: cytogenetic damage in lymphocytes. Int J Radiat Oncol Biol Phys 2000;47:793–8.
[15] Slonina D, Biesaga B, Swakon J, Kabat D, Grzanka L, Ptaszkiewicz M, et al. Relative biological effectiveness of the 60-MeV therapeutic proton beam at the Institute of Nuclear Physics (IFJ PAN) in Krakow, Poland. Radiat Environ Biophys 2014;53:745–54.
[16] Henry CM, Hollville E, Martin SJ. Measuring apoptosis by microscopy and flow cytometry. Methods 2013;61:90–7.
[17] Zhang G, Gurtu V, Kain SR, Yan G. Early detection of apoptosis using a fluorescent conjugate of annexin V. Biotechniques 1997;23:525–31.
[18] Koopman G, Reutelingsperger CP, Kuijten GA, Keehnen RM, Pals ST, van Oers MH. Annexin V for flow cytometric detection of phosphatidylserine expression on B cells undergoing apoptosis. Blood 1994;84:1415–20.
[19] Ghardi M, Moreels M, Chatelain B, Chatelain C, Baatout S. Radiation-induced double strand breaks and subsequent apoptotic DNA fragmentation in human peripheral blood mononuclear cells. Int J Mol Med 2012;29:769–80.
[20] Preckel T, Luedke G, Chan SDH, Wang BN, D'ubrow R, Buhlmann C. Detection of cellular parameters using a microfluidic chip-based system. JALA 2002;7:85–9.
[21] McCaman MT, Murakami P, Pungor Jr E, Hahnenberger KM, Hancock WS. Analysis of recombinant adenoviruses using an integrated microfluidic chip-based system. Anal Biochem 2001;291:262–8.
[22] Tilly JL, Hsueh AJ. Microscale autoradiographic method for the qualitative and quantitative analysis of apoptotic DNA fragmentation. J Cell Physiol 1993;154:519–26.
[23] Hosid S, Ioshikhes I. Apoptotic lymphocytes of H. sapiens lose nucleosomes in GC-rich promoters. PLoS Comput Biol 2014;10:e1003760.
[24] Zong WX, Thompson CB. Necrotic death as a cell fate. Genes Dev 2006;20:1–15.
[25] Weinlich R, Oberst A, Beere HM, Green DR. Necroptosis in development, inflammation and disease. Nat Rev Mol Cell Biol 2017;18:127–36.
[26] Linkermann A, Green DR. Necroptosis. N Engl J Med 2014;370:455–65.
[27] Somosy Z. Radiation response of cell organelles. Micron 2000;31:165–81.
[28] Kroemer G, Galluzzi L, Kepp O, Zitvogel L. Immunogenic cell death in cancer therapy. Annu Rev Immunol 2013;31:51–72.
[29] Nagata S, Tanaka M. Programmed cell death and the immune system. Nat Rev Immunol 2017;17:333–40.
[30] Roos WP, Thomas AD, Kaina B. DNA damage and the balance between survival and death in cancer biology. Nat Rev Cancer 2016;16:20–33.
[31] Pasparakis M, Vandenabeele P. Necroptosis and its role in inflammation. Nature 2015;517:311–20.
[32] Gameiro SR, Malamas AS, Bernstein MB, Tsang KY, Vassantachart A, Sahoo N, et al. Tumor cells surviving exposure to proton or photon radiation share a common immunogenic modulation signature, rendering them more sensitive to T cell-mediated killing. Int J Radiat Oncol Biol Phys 2016;95:120–30.
[33] Dewey WC, Ling CC, Meyn RE. Radiation-induced apoptosis: relevance to radiotherapy. Int J Radiat Oncol Biol Phys 1995;33:781–96.
[34] Amaravadi RK, Thompson CB. The roles of therapy-induced autophagy and necrosis in cancer treatment. Clin Cancer Res 2007;13:7271–9.
[35] Brauchle E, Noor S, Holtorf E, Garbe C, Schenke-Layland K, Busch C. Raman spectroscopy as an analytical tool for melanoma research. Clin Exp Dermatol 2014;39:636–45.
[36] Rieger AM, Nelson KL, Konowalchuk JD, Barreda DR. Modified annexin V/propidium iodide apoptosis assay for accurate assessment of cell death. J Vis Exp 2011.